KWARA STATE POLYTECHNIC, ILORIN.

DRIFT VELOCITY OF THE VIRTUAL HEIGHT OF IONOSPHERE.

BY:

ABDULRAHEEM OLAYINKA ABEEB
(ND/23/SLT/PT/722)

BEING A PROJECT SUBMITTED TO THE DEPARTMENT OF SCIENCE LABORATORY TECHNOLOGY, INSTITUTE OF APPLIED SCIENCES, KWARA STATE POLYTECHNIC, ILORIN.

IN PARTIAL FULFILLMENT OF THE REQUIREMENTS FOR THE AWARD OF ORDINARY NATIONAL DIPLOMA (OND) IN SCIENCE LABORATORY TECHNOLOGY (SLT).

JULY, 2025

CERTIFICATION.

This is to certify that this project is the original work carried out and reported by **ABDULRAHEEM OLAYINKA ABEEB (ND/23/SLT/PT/722)** to the Department of Science Laboratory Technology (SLT), Institute of Applied Sciences (IAS) Kwara State Polytechnic Ilorin and it has been approved in partial fulfillment of the requirements of the award of National Diploma (ND) in Science Laboratory Technology (PHYSICS ELECTRONICS UNIT).

----------------------------	**-------------------------------**
DR. AGUNBIADE G.	**DATE**
(Seminar Supervisor)	
----------------------------	**-------------------------------**
MR. LUKMAN I. A.	**DATE**
(SLT PT Coordinator)	
----------------------------	**-------------------------------**
DR. ABDULKAREEM USMAN	**DATE**
(Head of Department)	
------------------------------.	**-------------------------------**
EXTERNAL EXAMINER.	**DATE**

DEDICATION

To Almighty GOD who is kind and merciful to me.

To my father **Mr. ABDULRAHEEM** by and my mother **Mrs. ABDULRAHEEM** by whose encouragement, sacrifices, support and prayers I attained this level of success.

ACKNOWLEDGEMENT

I acknowledge the most-high God who has always been kind and merciful to me. I thank the Lord Almighty for the gift of life, sound health, and journey mercies and for providing all the needed resources throughout my period of studies. My profound gratitude goes to my beloved Supervisor, Dr. G. Agunbiade for his scholarly guidance and mentoring during the entire period of this work. I acknowledge and I appreciate the efforts of Dr. Usman for his contributions as the Head of Department of SLT. I appreciate, greatly, the current H.O.U. Mr. Sahahu Bashir who worked tirelessly to ensure that the needful is done. God bless you Sir.

Other members of academic and non-academic staff of Physics Department, Kwara State polytechnic Ilorin are highly appreciated. You are all unique and wonderful.

I am also indebted to my sibling. Your encouragement and voice of wisdom to me most especially when I share my challenges with you, are highly appreciated. I specially appreciate my beloved parents for their support and encouragement in the course of my education.

I love you all.

TABLE OF CONTENTS.

Contents

ABSTRACT.

Irregularity in the ionosphere, known as spread F, scatter radio signals causing degradation in radio communications. A proper understanding of the variation of spread F is therefore very useful in radio communication network design. However, the investigation of spread F with respect to vertical drift velocity of the F-layer will give a better understanding of the mechanism responsible for the spread. This will help in bridging the gap in the knowledge useful for the prediction of occurrence of spread F. This study investigated the occurrence of equatorial day and nighttime ionograms. The objectives were to: (i) investigate the characteristics of the day and nighttime ionograms., (ii) determine the virtual height and other parameter on the monogram; (iii) obtain F2 layer vertical drift velocity around the time of spread F occurrence.

Data from ILORIN digitonide stations geographical coordinate of 8.5°N to 4.5°E which its ionograms recorded by Digisonde were used for this study. The nature of ionograms were identified. The data are for the year 2010, a year of low solar activity. The drift velocities of the F2 layer were obtained by calculating the rate of change of virtual height (h´F2) of the F2 layer. The findings of the study were that:

CHAPTER ONE: INTRODUCTION

1.0. Drift Velocity and Virtual Height

VELOCITY, quantity that designates how fast and in what direction a point is moving. The terms velocity and speed give us an idea of how fast or slow an object is moving. Velocity is the rate of change of an objects positions with respect to time in a specific direction.

DRIFT VELOCITY? It is the average velocity acquired by a charged particle (like an electron or proton) in the body due to an electric field.

Virtual height and actual height of the ionosphere?
Actual height varies. Depends on the time of day, time of year and state of the sun. Generally accepted to start at 50km and stop at 1000km. **Virtual height** is the height of the reflecting layer such as would be measured using a radio-ionosonde and depends on the frequency being reflected (amongst other things).
Source: http://en.wikipedia.org/wiki/Ionosphere

The ionosonde also records the "virtual heights" of different layers in the ionosphere. They are called "virtual heights" as the **radio pulse** is assumed to travel at a constant speed, when in fact it slows near the critical frequency of the layer. Corrected heights are referred to as "true heights". "Virtual heights" are obtained from the time of flight of the transmitted radio pulse from transmitter, ionospheric reflection and back to the receiver.
http://www.ips.gov.au/HF_Systems/1/4
The highest frequency which the ionosphere will reflect vertically is called foF2. These foF2 measurements from various sites can be used to create a map of foF2.

Virtual Height of Ionosphere.

The Virtual height of the ionosphere can be described as the height of the reflecting layer and could be determined using a radio-ionosonde and depends on the frequency being reflected. Virtual heights could be explained as the radio pulse presumed to move at a uniform or constant speed when, in reality, it slows near the layer of the critical frequency. Virtual heights are gotten from the time of flight (TOF) of the transmitted radio pulse from the transmitter, ionospheric reflection and return to the receiver. The virtual height of the ionosphere of the F2 layer can be illustrated when the wave is gradually refracted down rather than sharply refracted. The refracted and incident rays below the ionized layer follow the same path as if the reflection has taken place from the high altitude. The spot can be termed virtual height or altitude of this layer. That is to say, when the incidence and rays coming back are extrapolated to a vertex they met at a height h, this is termed virtual height. The height or altitude, which is estimated by supposing that the waves move with the velocity of light known as the virtual height. (Akbar *et al.,* 2013). Gradual refraction in the ionosphere permits radio signals to be received in long distances.

GENERATION OF POST-SUNSET PLASMA BUBBLES

This night time irregularity is observable on nighttime ionograms within the low and equatorial latitude region of ionosphere. The Generalized Rayleigh-Taylor instability has been identified as the primary mechanism for the generation of post-sunset plasma bubbles which is the major initiator of spread F. It is triggered when the height of the F-layer reaches or surpasses a threshold. The lifting of the F-layer height is **caused** by the action of the vertical drift and lifting, which is most prominent after sunset due to the enhancement in the eastward electric field just before reversal called the pre-reversal enhancement (PRE). It is an irregularity which is noticed on ionograms when an ionosonde attempts to measure the reflection height of the F region. If this exercise is being done at the same time with the period of occurrence of this irregularity,

1.1. The Earth's Atmosphere

The atmosphere is an envelope of air and it comprises of a mixture of gases that serve as a protective guard for the earth and permit the existence of life. If not because of the atmosphere, one would have been ice-covered due to the very low temperatures at nighttime and burned due to the extreme heat from the sun during the period of the day.

1.2. Composition

Over 75% of the atmosphere comprises of nitrogen and oxygen. However, the 1% remaining contains a mixture of water vapor, ozone and carbon dioxide. It does not produce only essential weather characteristics, for example, cloud and rain. It also has an effect generally on the climate of the earth, through for instance, global warming and greenhouse effect.

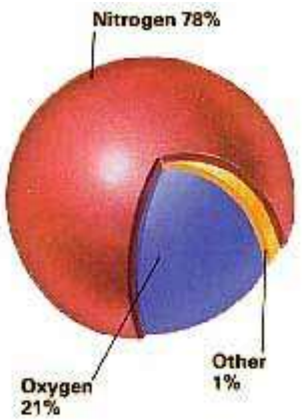

Figure1.1 The earth composition

(Source: https://www.scribd.com/presentation/139056296/Atmosphere)

Percentage composition of the constituent is as shown in the Table1.1 below.

Table 1.1 Percentage of the earth composition

Neon, Helium, Krypton	0.0001%
Argon (Ar)	0.93%
Oxygen (O_2)	20.95%
Nitrogen (N_2)	78.08%

1.3. Atmospheric Layers

The atmosphere has five layers grip by the force of gravity around the planet. Pressure in the atmosphere reduces quickly with altitude and the air temperature likewise vary, as one goes upwards across the layers. It is the variation in temperature, which separate it into the layers of atmosphere as explained below.

Troposphere

The layer nearest to the Earth is the troposphere which is about 11km high and can be almost 17km high in the tropics close to the equator. There would be no rain, clouds, and other weather features if there is no water vapor in the troposphere. The troposphere is where the air is continually moving and is not a stable layer. It is subjected to uneven ride known as turbulence. Temperature reduces with increase in height in the troposphere region, temperature drops about 6.5^{o}C for every kilometer above the surface of the earth. From the ground troposphere is heated up and the solar radiation absorbed is discharged as heat back in the infrared region. Tropospause divides the troposphere from the stratosphere. The air temperature in this region then reduces linearly with height.

Stratosphere

The stratosphere is the second layer of air above the earth's surface and stretches from heights of about 12km to an altitude of about 50 km. Ozone layer was discovered here. The ozone layer absorbs Sun's harmful radiations that are dangerous to animal life and plant. The ultraviolet radiation absorption from the sun by the atmospheric ozone layer triggers a temperature rise in the upper part of the layer. The temperature remains moderately constant in the lower part of the stratosphere.

Mesosphere

Mesosphere is 50km - 80km higher than the earth's surface. The air is very cold and thin beyond the stratosphere. In mesosphere, temperature reduces with increase in altitude as a result of reducing solar heating and increasing cooling by the carbon four oxide radiative emission.

Thermosphere

This is the fourth layer and it lies within 80km-110km higher than the earth. In this layer, temperature rises with altitude and it could reach a value ≥ 2000°C. As a result of the extremely low density of molecular constituents in the thermosphere, there is a temperature inversion in the region. Thus, radio signals travelling through thermometric region are reflected to the earth.

Exosphere

Satellites are stationed in the exosphere and this is found at the altitude of about 500 km. This is the layer and place where the atmosphere merges into space. .

The forms radiation causing ionization in the ionization could be summarized below:

REGION	PRIMARY RADIATION IONIZING FORMS
C	Cosmic
D	Hard X-ray, Lyman alpha
E	Extreme Ultra-Violet and Soft X-rays
F1	Ultra-Violet and Extreme Ultra-Violet
F2	Ultra-Violet

(Shows the forms radiation causing ionization in the ionization)

1.4. Statement of the Problem

Although a lot of work had been carried out on spread F since its first discovery by previous researchers. A lot questions are still not yet answered, some of the problems are yet to be dealt with through research includes. (i) The daytime ionograms have not been compressively studied in Ilorin. (ii) Calculating the vertical drift velocity of virtual height of ionosphere has not been studied. Ionogram data and spider date were compared. Also, there are limited published works on this in the African sector. As a result of this, there is a need for a clearer documentation of the appearance of these irregularities. A proper understanding of the variation of spread F is very useful in radio communication network and design.

1.5. The Aims and Objectives

This study is aimed therefore at investigating the day and nighttime ionograms within Ilorin. The objectives are to investigate:

(i) The study day and nighttime ionograms characteristics.

(ii) Determination virtual height of ionosphere and vertical drift velocity using ionograms and data obtained from spidar website.

1.6. Ionospheric Studies and Ionogram

Ionospheric Parameters

Ionospheric parameters are the parameters produced by Digisonde and displaced by an ionograms. A Digisonde is used to determine Ionospheric characteristics above the vicinity of the instrument. The Computer processing of the received radio waves is used to produce ionograms which are employed to determine the characteristics and parameters of the various ionospheric layers. The characteristics and parameters are shown in Table 2.1.

Table.2.1 Ionospheric characteristics deduced from Digisonde measurements.

Names	Descriptions
foF2p	Predicted value of foF2
foF1p	Predicted value of foF1
foEp	Predicted value of foE
foF2	F2 layer critical frequency
foF1	F1 layer critical frequency
foE	E layer critical frequency
hmF2	Peak height F2-layer
hmF1	Peak height F1-layer
hmE	Peak height of E-layer
h`F2	Minimum virtual height of F2 trace
h`F	Minimum virtual height of F trace
h`E	Minimum virtual height of E trace
M(D)	MUF(D)/foF2
B0	IRI thickness parameter
B1	IRI profile shape parameter
scale F2	Scale height at the F2-peak
TEC	Total electron content
foEs	Es layer critical frequency
h`Es	Minimum virtual height of Es trace
fminEs	Minimum frequency of Es-layer
fmin	Minimum frequency of ionogram echoes
fminE	Minimum frequency of E-layer echoes
fxI	Maximum frequency of F trace
fminF	Minimum frequency of F-layer echoes
MUF(D)	Maximum usable frequency for ground distance D
D	Distance for MUF calculation
h`Ea	Minimum virtual height of auroral E-layer trace
QF	Average range spread of F-layer
FF	Frequency spread between fxF2 and fxI
FE	Frequency spread beyond foE
QE	Average range spread of E-layer
foP	Highest ordinary wave critical frequency of F region patch trace
h`P	Minimum virtual height of the trace used to determinate foP
fbEs	Blanketing frequency of Es-layer
type Es	Type Es
dlt foF2	Adjustment to the scaled foF2 during profile inversion
foEa	Critical frequency of auroral E-layer

(Source: https://orbi.ulg.ac.be/bitstream/2268/87604/1/TN-RMI-2010-02_DB049%20Ionosonde%20Database.pdf)

(http://www.g0lfp.com/ionograms/ursi_codes.html)

DEFINITION OF SOME IONOSPHERIC CHARACTERISTICS AND PARAMETERS.

Top frequency of a layer: This is the highest frequency in which an echo trace is obtained from the layer at vertical incidence (weak discontinuous traces are ignored)

The Blanketing frequency of a layer: This is the lowest frequency in which the layer starts to become transparent. This is normally identified by the appearance of echoes from a layer at higher heights.

Critical frequency: This is the highest frequency in which the layer reflects and equally transmits. This discloses that the Layer critical frequency at all times lies between its frequency and blanketing frequency. It is also a maximum frequency that a radio wave can be vertically transmitted and still be refracted back to the earth.

Minimum virtual height: Minimum virtual height is the height at which the trace is horizontal. For a thick layer this can only occur if there is a lower thick layer causing group retardation which balances the change of virtual height with frequency due to the reflecting layer. In all these cases virtual minimum height is above the true height.

Maximum usable frequency (MUF): This is a propagation concept which is regarded as the highest frequency for Ionospheric transmission over an oblique path.

Operational Maximum usable frequency (MUF): This is regarded as the highest frequency that permits acceptable operation between the given points at given time and under stated or specified working conditions.

Classical MUF: This is defined as the highest frequency that can be propagated by a particular mode between specified terminals by ionospheric refraction only. It can be experientially determined as the frequency at which the high- and low- angle rays merge into a single ray.

Standard MUF: This s an approximation to the classical maximum MUF that is acquired by utilization of the ordinary transmission curve to vertical incidence ionograms together with the utilization of distance factor.

Maximum observed frequency MOF: Is the highest frequency that can be detected on an oblique incidence Ionogram. Total Electron Content is also an important ionospheric parameter.

1.7.The Digisonde

Digisonde is a present day computerized equipment used to obtain Ionospheric characteristics over the environs of the equipment. Digisonde has a radio wave, receiver, transmitter, associated receiving and transmitting antennas. Digisonde usually works within the 1 - 20 MHz band with a physically big transmitting antenna and four smaller, spaced receiving antennas installed in an equilateral triangle (the fourth antenna being positioned at the centroid of the triangle). Computer processing unit of the radio waves received is used to produce ionograms which are employed to obtain the characteristics of the different layers of ionosphere.

Digisonde Mode of Operation

In the ionosphere, a Digisonde can be compared to a radar. A radio wave is transmitted by a radar and then listens with a receiver matched for reflected radio waves from targets inside the radar beam. Generally, Radars, especially, for example, those used for control of air traffic, are manufactured to track and detect hard targets, that is., an airplane. As soon as the Digisonde transmitted frequency matches the ionospheric plasma frequency, the transmitted radio waves will reflect and return to the receiver of the Digisonde. The target of the Digisonde at the radar analogy are the free electrons in the ionosphere. The radio wave transmitted takes time (the time of flight) to go to the ionosphere and come back to the receiver upon reflection. Twice the virtual range to the ionospheric target and the radio wave frequency are received in connection with the ionosphere's number density. As the frequency is being swept by the transmitter, time of flight combinations (virtual range) and (electron number density) frequencies reflected characterize layers of ionospheric but the ionosphere atmosphere are not vacuums, remember that light goes at 3 X 108 m/sec in a vacuum. To get the true altitudes of the corresponding densities of electron number, corrections should be made to the measured or calculated virtual ranges.

The ionosphere is not going to be an effective target for the transmitted radio waves of the Digisonde at frequencies greater than the highest maximum electron number density (ionospheric plasma frequency). These higher transmitted radio waves of the Digisonde are not reflected to the receiver and keep on to travel in a line of sight (LOS) manner into the far places in space. The radio wave propagation through a magnetic field splits the radio wave transmitted into an extraordinary wave with a frequency different from the original and an ordinary wave with the original frequency. The frequency difference between extraordinary wave and ordinary wave is just about one-half the orbital electron frequency about the magnetic field line of the earth. The Digisonde digital nature makes modern radar processing methods to be used to enhance signal gain, generate several receive beams within the bigger transmit beam to assess ionospheric motions, to determine the direction of arrival, avoid interference, enable near real time and avoid interference, calculation of true-height electron density profiles and automatic scaling of multi-parameter ionospheric characteristics. (Source: http://www.gi.alaska.edu/instruments/digisonde)

The Figures in 2.1a, 2.1b, 2.1c, are the Digisonde portable sounder (DPS), Transmitting and Receiving antennas of the University of Ilorin. Digisonde Portable Sounder installed in Ilorin was produced by the University of Massachusetts Lowell Center for Atmospheric Research. The system makes up for a low power transmitter and equipped for measuring overhead ionosphere and gives real time data acquisition, processing of signals, control, display, storage and automatic analysis of data to define radio signal propagation. This is used to support surveillance operations or communications and enhance efforts on ionospheric research storage, signal processing, the acquisition of data, control, display and data analysis functions were upgraded into a single multi-tasking, while the analog circuitry had been condensed, multiple processor computer system.


.

Fig. 1.1a : The Digisonde portable sounder (DPS).

Figure.1.1b　　Figure.1.1c　　Figure.1.1d

A Transmitting antenna　　4 Receiving antennas　　A Global Positioning System

(a) The Digisonde portable sounder and the display unit, (b) The transmitting antenna, all from the University of Ilorin, Nigeria Digisonde station (c) The Magnetic Loop Turnstile antenna with attached preamp module, and. (d) Global Positioning System.

It has been made simpler by the utilization of low power transmitter, wide bandwidth devices, and available commercially PC expansion boards. Currently, one of the major applications for the real-time data generated by digital ionospheric sounders was to manage the operation of high frequency (HF) networks and channels. Another fundamental objective of the DPS development is the storage of the data created by the system in an easily accessible format. . . (http://www.digisonde.com/instrument-description.html)

The Global Positioning System (GPS)

The global positioning satellite system (GPS) is a global navigation satellite system and space-based device. At any place on or near to the earth, it supplies time and location information in all the weather, where there is a clear line of sight to at least four or more global positioning satellites.

1.8. Ionogram

The presentation of the data generated by an ionosonde is called Ionogram. It is the virtual height graph of the ionosphere plotted versus frequency. Data generated or information from ionograms may be utilized to get the variations in the earth's ionosphere due to space weather events.

Description of the Ionogram

From Figure 2.2 Ionogram demonstrates a fully-developed F layer with an ionization peak at about 220 km. There is also a height of E layer of about 110 km. The Ionogram displays clearly how the transmitted signal from digisonde breaks into reflected extraordinary waves and into reflected ordinary. The parameter of foF2 and the ionogram graph in the list at the left hand side of the graph. The topmost frequency displayed would be reflected from the ionosphere for vertical incidence is 4.8 MHz. That is where a radio wave coming from the ground. What seems to be faint reflections from height of 425 km were displayed by the ionogram. Actually, the product of the sounder's radar signal being reflected by the ionosphere are these graph points. Going back to the ground from where they had reflected back to the ionosphere for a second reflection before being detected by the receiver of the Digisonde. The time of flight (TOF) is therefore doubled the normal reflection and the computed virtual altitude doubles the normal virtual altitude.

Under low conditions of ionospheric absorption this type of presentation is frequently seen. Figure 2.2 is a typical ionogram sample. It shows clearly the double hop extraordinary and ordinary frequencies and virtual ranges. Light blues indicate ionospheric reflection, green are the locus of the received extraordinary frequencies and their corresponding virtual ranges. Black line is scaled by digisonde computer plasma frequency (electron density) versus virtual height. Red lights are locus of the received ordinary frequencies and their corresponding virtual ranges, the second black curve line is the Digisonde computed plasma frequency (electron density) versus true height.

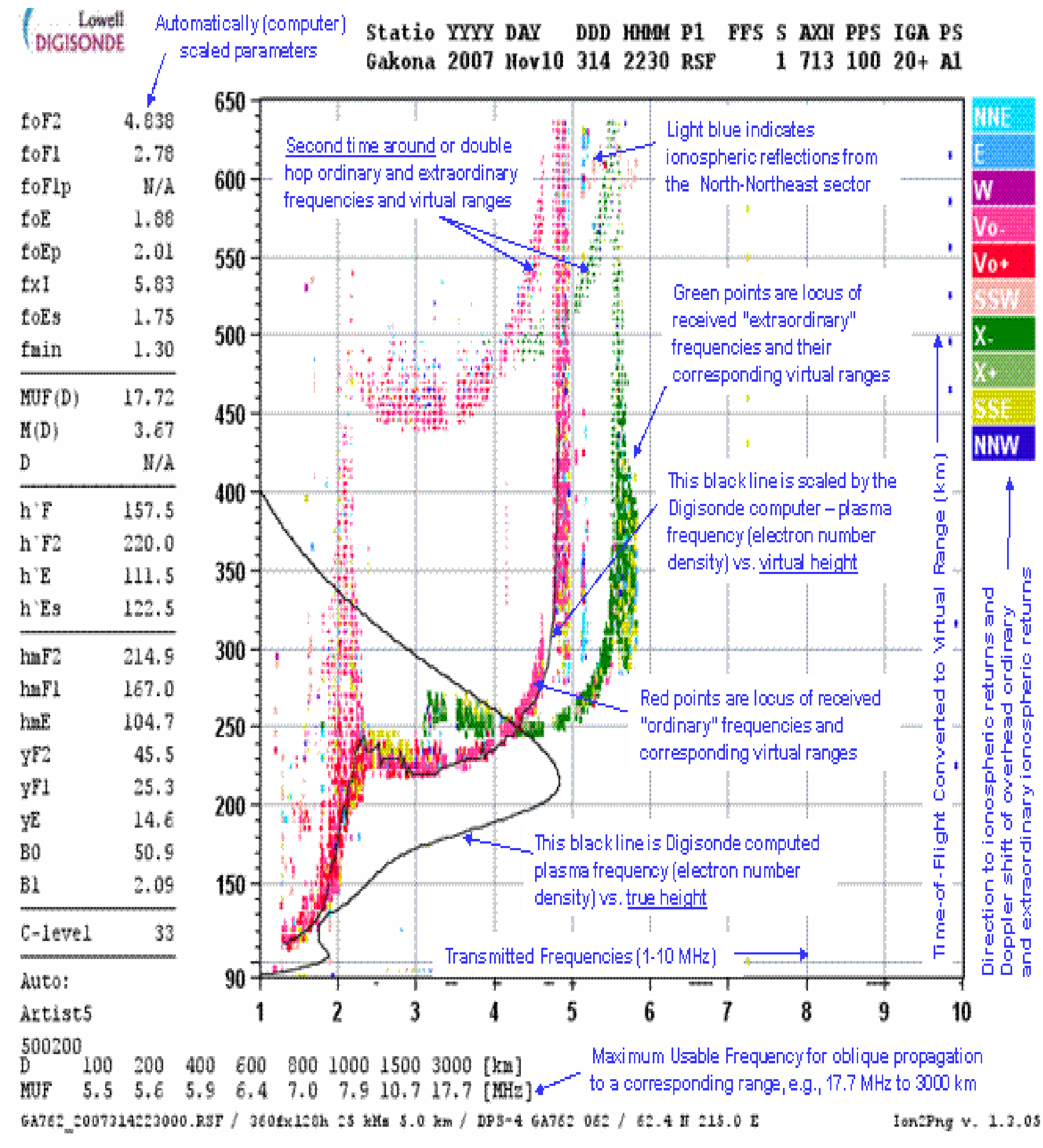

Figure 2.2 (typical ionogram) Source: (http://www.gi.alaska.edu/instruments/digisonde) (http://www.g0lfp.com/ionograms/ursi_codes.html)

1.9. Literature Review On Spread F and Vertical Drift Velocity Studies.

For several decades the phenomenon of ionograms has been studied. A spread in the virtual altitude of the normally smooth ionograms of the post sunset ionosphere was first presented by Booker & Wells (1938) using ionosonde. The following present the summary of different results by different authors on the study of equatorial spread F.

(i) Abdu (2012) worked on the *Quiet* time variability and ESF development under solar minimum condition. The work gives a short review on the understanding of ESF irregularities throughout the solar minimum and the sunset electrodynamics process which triggers spread F occurrence was explained. The function of the sunset PRE in the vertical drift compared with to gravity wave precursor seed and ESF development is the instability growth and this vary with solar activity. ESF occurrence pattern depends greatly on gravity wave distribution throughout the solar minimum condition than solar maximum.

(ii) Manju *et al.,* (2007) study was based on the seasonal variations of the threshold altitude for the occurrence of equatorial spread F at the period of solar maximum and minimum years. The study investigated occurrence of the base side equatorial spread F (ESF) and its reliance on the polarity and magnitude of the thermospheric meridional wind just before occurrence of ESF during equinox and winter seasons of solar maximum, summer in year 2002 and minimum years 1995, Ionosondes data from TRV (8.5^0 N, 76.5^0E, dip=0.5^0N) and SHAR (13.7^0 N, 80.2^0E, dip 5.5^0N) longitude sector were used. Study investigated the changes in the threshold altitude of the base of the F layer for the triggering of ESF, regardless of the magnitude and polarity of the meridional winds during the periods above. The study shows that the threshold height above which ESF triggering is completely controlled mainly by the collisional R-T instability.

(iii) 15minutes ionograms at Kodaikanal 10.2^0N; 77.5^0E; dip 4^0N were studied in the northern summer months May to August. 1994 and 1995 to determine the ambient ionospheric conditions against the presunrise start of spread-F takes place. A 38 night with midnight start of Spread-F and 34 nights without spread-F were used. It was discovered that a noticeable rise in F layer altitude, starting around 2100 LT, appears on nights with Spread-F as well as without Spread-F. This characteristic is being seen in the nighttime pattern of height of F layer on many separate nights along with the average height of F layer for the two groups of nights. The result convincingly recommends that the height of F layer does not play an essential role in the midnight spread-F onset throughout the June solstice of solar minimum.

(iv) MacDouga *et al.,* 1998, studied Presunrise spread F at Fortaleza. The work reveals that the research was carried out in Fortaleza Brazil situated in the equatorial region. Maximum spread F occurrences were noticed during sunspot minimum, especially during December solstices. The results showed that these bottomside bulges are unstable as a result of gradient-drift instability that was slowly growing and generated spread F. The bulges prove to the evidence of a Rayleigh-Taylor process.

1.10. Rayleigh Taylor instability (RTI)

The RTI process is the physical mechanism for the formation of ESF (Dungey 1956). RTI can be explained as the interpenetration of materials that occurs whenever a light fluid pushes on a heavy fluid (Rayleigh, 1883 and Taylor, 1950). Rayleigh Taylor instability is a process which is dynamic whereby the two fluids seek to reduce their combined potential energy. RTI is the description of the instability of the interface connecting two different fluids in which both of the fluids have different densities. When this happens, the lighter fluid pushes the heavier fluid. (Chakrabarti

& Lakhina 2003) The Rayleigh-Taylor instability is a fundamental fluid-mixing mechanism. (http://www.globalsecurity.org/wmd/intro/rayleigh-taylor-instability.htm) RTI develops when heavier plasma is supported by the lighter plasma, which is exactly the case at the time of post sunset F-region ionosphere. Generally, at the magnetic equator, around the post-sunset, the conditions required for the RTI are met, where the base side of the ionospheric F-layer has recombined and the whole F-layer itself is already raised appreciably and noticeably by the PRE in the eastward electric field. A very sharp vertical density gradient is generated by this, which is not stable to vertical perturbations in the ionosphere. This is usually occurs when a fluid which of high-density is situated on top of a fluid which of low low-density in a gravitational field. At the fluid interface, any fluctuation will allow gravity to pull the fluid of high-density downwards so that the fluid of the low-density ends up on top and this is an interchange of the two fluids. (Narayan 2007). The RTI theory involves a vertical plasma density gradient with dense F-region plasma over less dense E-region plasma, enhanced by the steeping of the bottomside at night. This gradient, when perturbed, will generate polarization electric fields that grow the perturbation through EXB plasma drift. This is the situation in the post sunset equatorial ionosphere just below the F-region. The D and E regions disappear due to recombination after sunset steepens the bottomside and prevents the shorting of the F region currents. We can approximate the layer below the F-region as a vacuum in terms of plasma density with heavy fluid supported by the lighter one.

The electrons and ions drift in opposite directions. Based on this random thermal motion of electrons and ions, a ripple develops along the interface. A further increase in the drift velocity will cause the ripple to grow and they cause a charge build up on the side of the ripple. An electric field E develops, which changes the sign from crest to trough in the perturbation wave. The E×B drift is always upward in the upper surface of the ripple and is downward in the lower region of the ripple. As a result, the ripple becomes unstable producing the small-scale irregularities. As they rise, these irregularities spread out towards the magnetic field lines in north and south. The F-region fields cause the F-layer to rise at higher altitude, which reduces the collisions rate between the charged particles and the neutral species, and hence, the E-region conductivity, which then enhances the R-T growth rate for example, Balsley *et al.*, 1972. PRE is known to be responsible for a sudden rise in the vertical plasma drift in the F-region,

CHAPTER TWO: DATA AND METHODS

2.0. Data and Methods

2.1. Data and Approach.

The data used for this study were ionograms for the year 2010, a year of low solar activity. The ionograms which were archived in DIDBASE were downloaded online from https://lgdc.uml.edu/common/DIDBFastStationList. Spider data was also used. Digisonde station geographical coordinate 8.5°N to 4.5°E (ILORIN), located at the equatorial ionisation anomaly (EIA) region, was used for the study. This includes data from Ilorin station, which has not been used before for such study. Variation (increase or decrease) in virtual height (h´F2) of F2 layer with respect to time at 15-minute interval from post sunset till the first appearance of spread F on the ionograms were recorded, the value of the h´F2 were then used to compute vertical drift values using the relation

$\Delta h/\Delta t = \frac{\Delta \text{h}'\text{F2}}{\Delta \text{Time}}$. The ionograms observed at hourly interval for occurrence and those of fifteen-minute interval for drift velocity were converted to local time (LT). For better analysis and consistent trend in result analysis, the stations were arranged in order of increasing dip latitude. Ionograms with appearance of spread F were identified and the type of Spread-F, that is, range spread F, frequency spread F and mixed spread F were noted against the time of occurrence. The occurrence percentage of spread F was calculated from the ratio of the number of days with Spread-F to the total number of days with data.

$$\%\ of\ occurrence\ = \frac{number\ of\ ionograms\ with\ spread\ F}{total\ number\ of\ ionograms} x100$$

The list of the stations and their respective geographic, geomagnetic coordinates as well as dip latitudes are shown in Table 3.1.

Table 3.1: Coordinates of the stations studied.

Station Nme	Geog Latitude	Geog Longitud	Geomag Latitude	Geomagc Longitud	DIP Latitude	TIME ZONE
ILORIN	8.5°N	4.5°E	10.6°N	78.36°E	7.867°S	(UTC/GMT +1 HOUR)

The abbreviations used in Table 3.1 for the stations shall be used in result presentation and discussion.

2.2. Ionogram Samples

The figures below show samples of ionograms obtained from each of the stations showing different types of spared F.

2.2.1. Ilorin Ionogram Samples

ILR: (UTC+01:00)

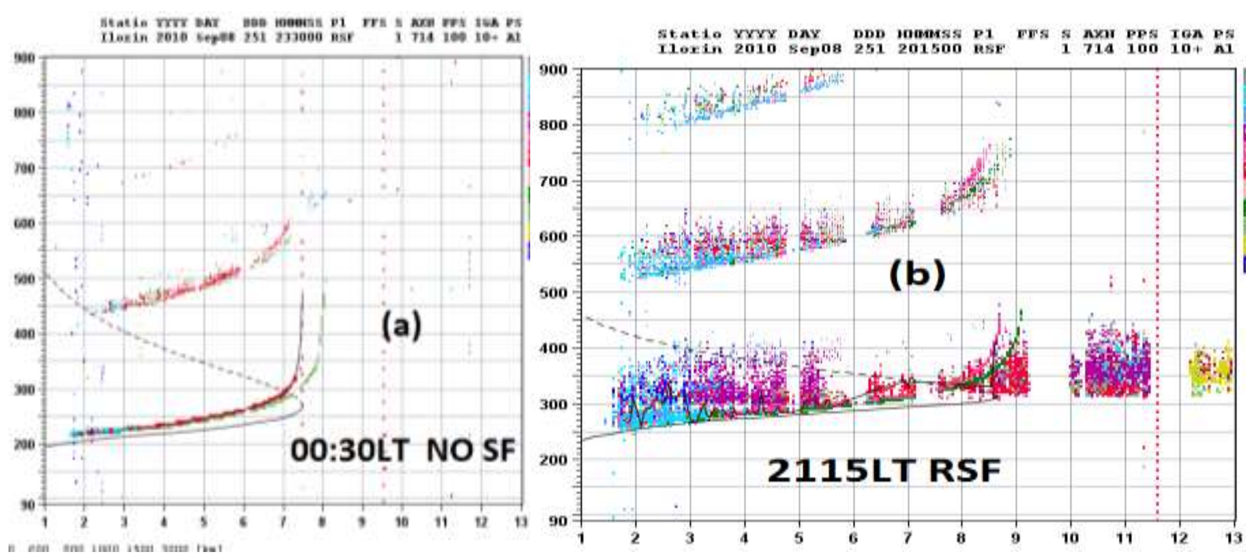

Fig.3.3 (ILR) (a) NO SF, (b) RSF

CHAPTER THREE: RESULTS AND DISCUSSION

3.0. Results and Discussion

The results obtained in this study are presented and discussed in this chapter.

3.1. Vertical Drift Velocity

The vertical drift velocity during the post sunset hours is displayed in Table 3.13, Table 3.14 and Figure 4.25-30. The rate of change in virtual height (h´F2) of F2 layer with respect to time from post sunset till the time of first appearance of spread F on the ionograms was observed at hourly interval. The vertical drift velocity of F2 layer (h´F2) was obtained from the rate of change of h´F2 with respect to time. That is, $\Delta h \Delta t = \frac{\Delta \text{h}'\text{F2}}{\Delta \text{Time}}$ and it is expressed in m/s/. For example, in Table 4.13 a (KWJ on 5-Apr) and Table 4.11 b (KWJ on 2-Apr-) were calculated respectively. (Table 4.13 a) = (C111-C107)*1000/60*60) =(370-225) *1000/(60*60) =**40.2777** and (Table 4.13 b) = (C45-C41)*1000/(60*60) = (285-260) *1000/(60*60) = **6.944444**. For instance, one hour vertical drift velocity at the time occurrence in Table 4.13b on 2-Apr-10 at 2045LT is 6.9444m/s. The overall results obtained from Table 4.13 and Table 4.14 show that one-hour vertical drift velocity at the time occurrence is within 3m/s to 40 m/s during the equinox period and 3m/s to 18 m/s during the solstice period. When the same procedure is applied in Table 4.13a from 1915LT to the time of occurrence at 2115LT, the vertical drift velocity ranges between -8m/s to 40.27m/s. In general, in this work, one hour vertical drift velocity from post sunset till the time of the first appearance of spread F occurrence taken at fifteen minute intervals as it was calculated in Table 4.13 and Table 4.14 the overall result is between -17m/s to 40.27m/s in the equinox months and is -10.m/s to 29m/s in the solstice months.

High value of average drift velocity shows how consistent or regular and continuous increase in virtual height towards occurrence window. Low or negative value of average drift velocity shows inconsistence increase or decrease in virtual height at hourly interval towards occurrence window. High initial virtual height, after post sunset, usually requires a few numbers of vertical drift velocity before the spread F occurrence is triggered. One-hour drift velocity at the point of occurrence must have a noticeable value and should not be negative value if it has not attained a minimum height of occurrence before that period. Positive or high value of average drift velocity is an indication or a probability that spread F will occur. When virtual height begins to rise after post sunset with low initial virtual height and there is consistent increase and it eventually attain high height occurrence, then the average drift velocity will also be high. High initial virtual height requires little vertical drift velocity and consistent virtual height increase but average drift velocity might be low as well. For any day without spread F occurrence, it is either the average drift velocity is very low or less or equal to zero.

Table 4.13 show hourly vertical drift velocity till the point of spread F occurrence.

S/N	5-Apr-2010	(a)		M/S
	TIME	h´F2	OCCUREENCE	VELOCITY
98	18:00	240	NIL	4.166666667
99	18:15	265	NIL	73.61111111
100	18:30	255	NIL	#VALUE!
101	18:45	252	NIL	#VALUE!
102	19:00	248	NIL	2.083333333
103	19:15	255	NIL	-2.77777778
104	19:30	248	NIL	-1.85277778
105	19:45	232	NIL	-5.55555556
106	20:00	235	NIL	-3.47222222
107	20:15	225	NIL	-8.33333333
108	20:30	240	NIL	-2.31388889
109	20:45	250	NIL	5.091666667
110	21:00	255	NIL	5.555555556
111	21:15	370	SF	40.27777778

S/N	2-Apr-2010	(b)		M/S
	TIME	h´F2	OCCUREENCE	VELOCITY
34	18:00	245	NIL	2.777777778
35	18:15	250	NIL	69.44444444
36	18:30	247	NIL	#VALUE!
37	18:45	250	NIL	#VALUE!
38	19:00	250	NIL	1.388888889
38	19:15	250	NIL	0
40	19:30	253	NIL	1.85
41	19:45	260	NIL	2.777777778
42	20:00	265	NIL	4.166666667
43	20:15	272	NIL	6.019444444
44	20:30	273	NIL	5.555555556
45	20:45	285	SF	6.944444444

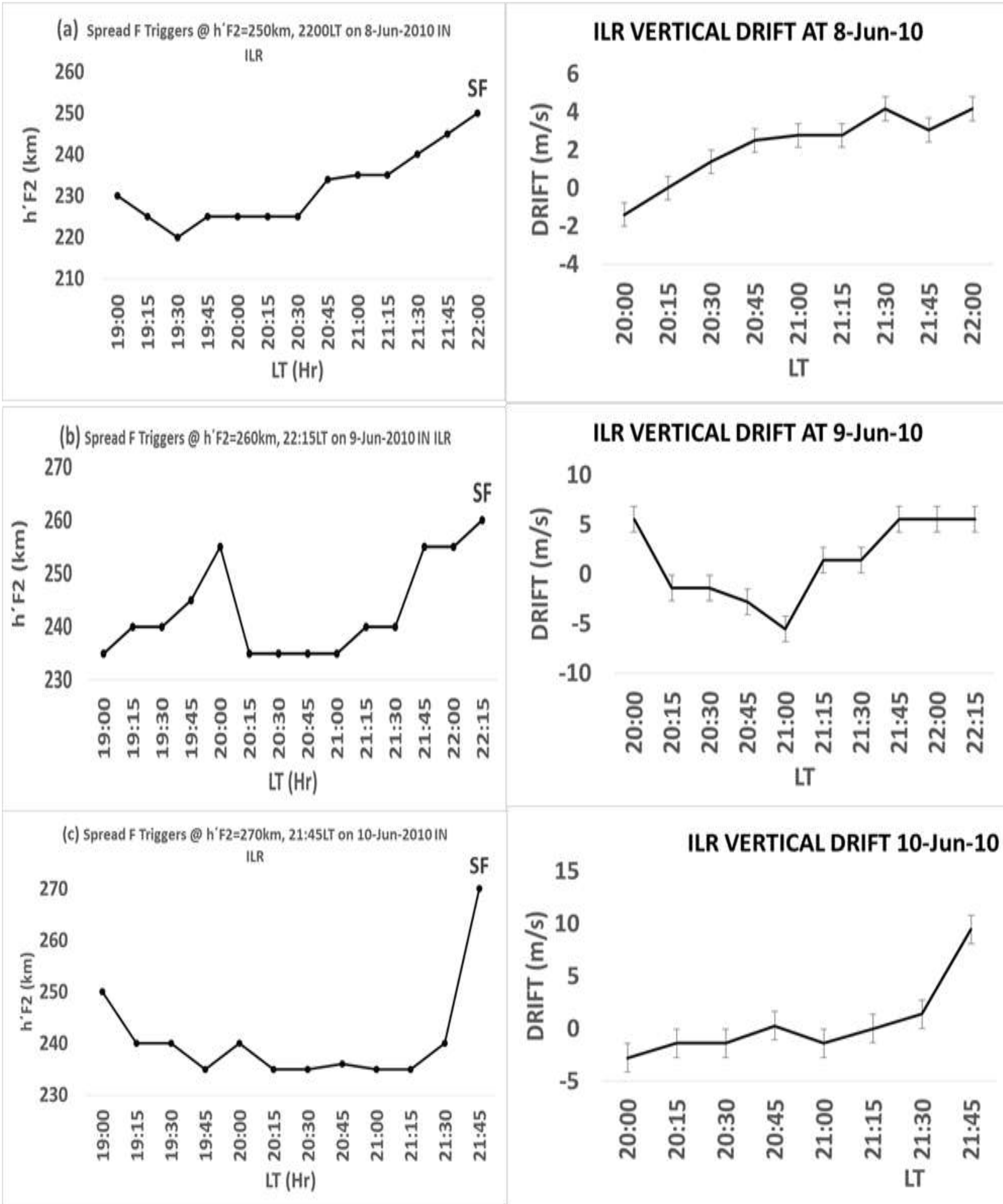

Figure 4.28 shows Variation of h´F2 with LT **(Left panel)** and corresponding **Vertical** drift velocity (**Right panel)** in June in **ILR**

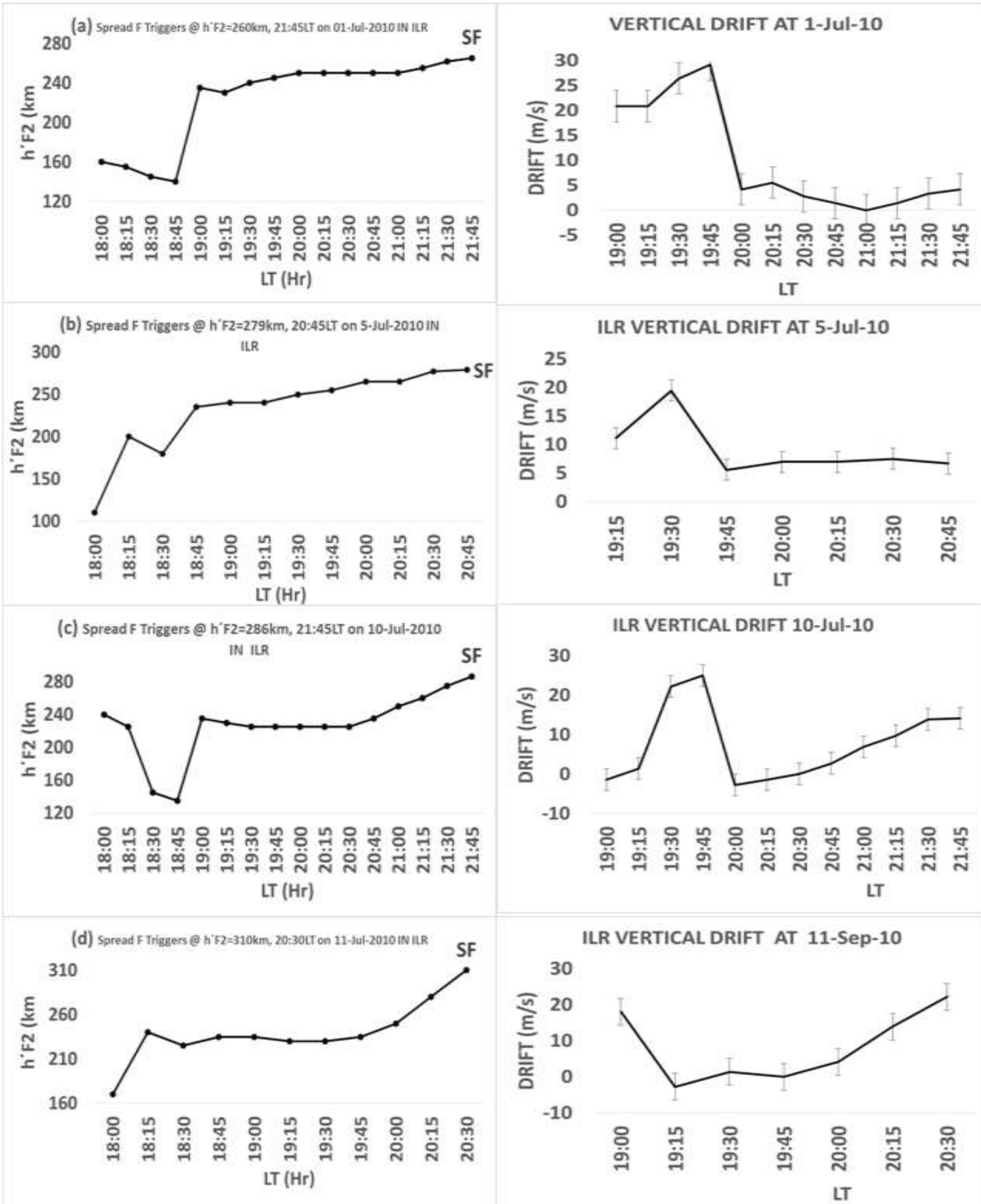

Figure 4.29 shows Variation of h´F2 with LT **(Left panel)** and corresponding **Vertical** drift velocity (**Right panel)** in July in **ILR**

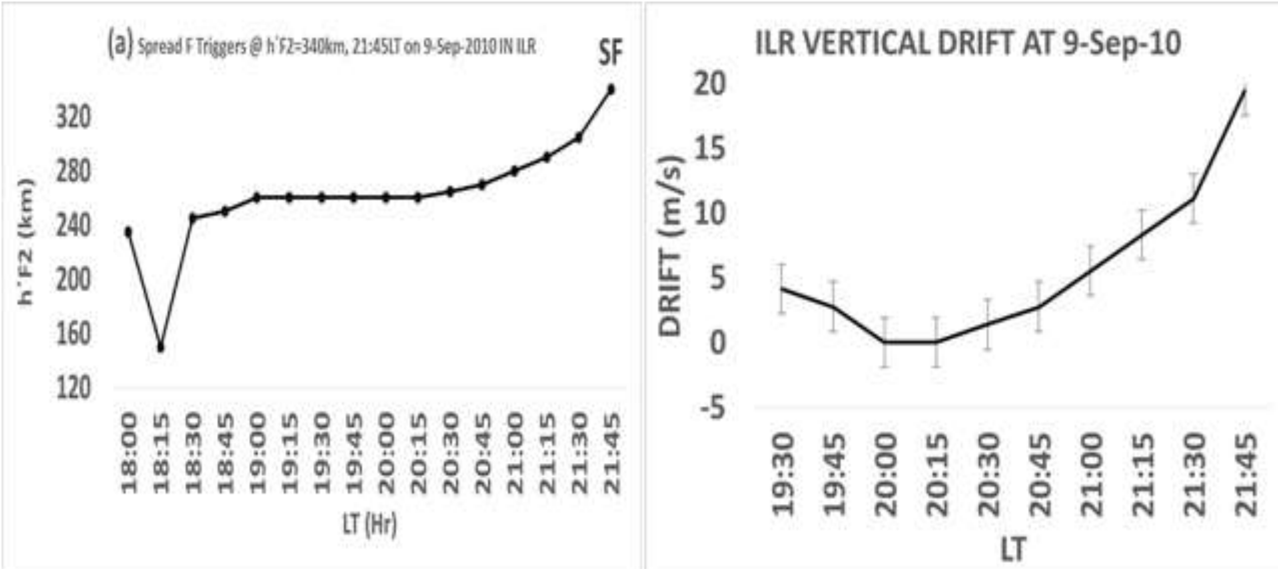

Figure 4.30 shows Variation of h´F2 with LT **(Left panel)** and corresponding **Vertical** drift velocity (**Right panel)** vertical drift velocity in Sept in ILR

Table 4.14d-f show hourly vertical drift velocity sample calculated at stipulated time in the table.

One Hour Vertical Drift Vel at	1-Jun-10	8-Jun-10	9-Jun-10	10-Jun-10	17-Jun-10
20:00	5.56	-1.39	5.56	-2.78	1.39
20:15	**8.33**	0.00	-1.39	-1.39	0.00
20:30		1.39	-1.39	-1.39	6.94
20:45		2.50	-2.78	0.28	**9.17**
21:00		2.78	-5.56	-1.39	
21:15		2.78	1.39	0.00	
21:30		4.17	1.39	1.39	
21:45		3.06	5.56	**9.44**	
22:00		**4.17**	5.56		
22:15			**5.56**		
22:30					
22:45					
	(d) ILR JUNE				

One Hour Vertical Drift Vel at	1-Jul-10	5-Jul-10	10-Jul-10
19:00	20.83	36.11	-1.39
19:15	20.83	11.11	1.39
19:30	26.39	19.44	22.22
19:45	29.17	5.56	25.00
20:00	4.17	6.94	-2.78
20:15	5.56	6.94	-1.39
20:30	2.78	7.50	0.00
20:45	1.39	**6.67**	2.78
21:00	0.00		6.94
21:15	1.39		9.72
21:30	3.33		13.89
21:45	**4.17**		**14.17**
(e) ILR			

One Hour Vertical Drift Vel at	5-Sep-10	6-Sep-10	8-Sep-10	9-Sep-10	10-Sep-10
19:00	1.39	23.61	4.17	6.94	5.56
19:15	2.78	27.78	23.61	30.56	5.56
19:30	5.56	5.56	-1.39	4.17	6.94
19:45	6.94	6.94	-1.39	2.78	9.72
20:00	11.11	9.72	-1.39	0.00	11.11
20:15	8.33	18.06	1.39	0.00	12.50
20:30	**4.17**	**19.44**	4.17	1.39	16.67
20:45			**6.94**	2.78	13.89
21:00				5.56	15.28
21:15				8.33	**11.11**
21:30				11.11	
21:45				**19.44**	
22:00					
	(f) ILR SEPT				

3.2. . Discussion

3.1. Vertical Drift Velocity

The vertical drift velocity during the post sunset hours is displayed in Tables 4.13 - 4.14 and Figure 4.24-30. The rate of change in virtual height (h´F2) of F2 layer with respect to time from post sunset till the first appearance of spread F on the ionograms were observed at hourly interval. The vertical drift velocity of F2 layer (h´F2) was obtained from the rate of change of h´F2 with respect to time as well. It discovered that high value of average drift velocity shows how consistent or regular and continuous increase in virtual height towards occurrence window. Low or negative value of average drift velocity shows inconsistent increase or decrease in virtual height towards occurrence window**.** Drift velocity must be noticeable depending on least virtual height after the post sunset or during the occurrence window and it must not be negative value, if it has not attained a minimum height of occurrence. The positive or high value of average drift velocity is an indication or is a probability that spread F will occur.

When virtual height begins to rise after post sunset with low initial virtual height and there is consistent increase and it eventually attains high height occurrence, then the average drift velocity will also be high. High initial virtual height requires little average drift velocity and consistent virtual height increase, but an average drift velocity might be low as well. Any day, without spread F occurrence, it is either their average drift velocity is very low or less or equal to zero.

The average drift velocity in ILR is June is between 3m/s - 9.17m/s, July is 4.11m/s - 14.16m/s and September is 3m/s - 19.44m/s Meaning that average drift velocity is higher during the equinoxes than solstice periods.

Our result is in conformity with Fejer 1999. When the upward drifts are greater than approximately 5-10 m/s near solar minimum, narrow unsteady layers of weak irregularities are formed in the lower F region in all seasons. He stated further that for upward drift velocities higher than -15-20 m/s, the unsteady layer is raised to heights where the gravitational drift term dominates in the Rayleigh-Taylor instability growth rate leading to strong and wide scattering regions. The upward drift, velocity drifts and layer height are necessary for the generation of spread F increase with solar activity. For example, peak upward velocity drifts of 40-45 m/s are required for the formation of strong spread F. The vertical plasma drifts play a dominant role on the evolution and generation equatorial spread F irregularities. The dependence of these irregularities on local time, season, and magnetic activity can be largely clarified and illustrated by corresponding effects on the night time and evening vertical drifts. The result above supports the conclusions of Basu *et al.* (1996), who suggest that post sunset upward drift velocity enhancement of the order of 10m/s - 20 m/s are necessary and required for the occurrence of spread F over Peru during equinox solar minimum. (Fejer & Scherliess 1999).

The crests equatorial anomaly in TEC are closer to the magnetic equator in the June solstice period, which implies that the daytime, upward E×B velocities drifts are smaller in the June solstice than in the Equinox. Anderson *et al*, 2009 is in agreement with our result. A threshold velocity and a height of the ionosphere were proposed to produce positive Rayleigh-Taylor Instability growth rates, and this threshold was discovered to change with solar flux. (Fejer *et al*. 1999 & Stolle *et al* 2008. The pre-reversal vertical velocity drift in the equinox is larger than the period of the solstice, with a lower value (smooth averaged) up to 25 m/s (30 m/s). The maximum pre-reversal drift velocity nearly reaches 45 m/s. The equinoctial peak velocities vary between about 35m/s and 45 m/s. (Li *et al* 2008). These are in perfect agreement with this research.

CHAPTER FOUR: CONCLUSION AND RECOMMENDATIONS

4.0. Conclusion and Recommendations

4.1. Conclusion

Spread F is the irregularity in the F region of the ionosphere which scatter radio signals causing degradation in radio communications. The results obtained from the work are summarized as follows:

(i) Spread F occurs between 1900LT and 0600LT and occurrence frequency varied between 0.13% and 40.71%. ILR in August at 0100LT-0200LT, in September 2300LT -2400LT and in October at 2200LT – 2300LT.

(ii) Spread F is triggered when the virtual height of F layer is within 250km and 370km during the post sunset period at (1900LTand 2300LT). The duration of occurrence ranges between 5 to 12 hours

(iii) Spread F occurred when there is continuous and a noticeable rise in virtual height and the height of the F2 layer is at least 250km. The average drift velocity is within 3m/s - 40m/s during the equinoxes and .3m/s - 18m/s during the solstice months. The layers begin to rise around 1800LT – 1900LT in most of the stations, layer rises earlier in the equinox months and earlier occurrence during the equinox months. The high value of average drift velocity shows how consistent and regular continuous increase in virtual height towards occurrence window. Low or negative value of average drift velocity shows inconsistence increase or decrease in virtual height towards occurrence window. High initial virtual height during post sunset usually requires a few numbers of the drift before the occurrence. Low or negative average drift velocity is usually experienced on non-spread F occurrence days.

(iv) The occurrence frequency, height of occurrence and average drift velocity at the time of occurrence are higher during the equinoxes than the solstice months. This implies that all the attributes of the equatorial spread F are seasonally dependent.

(v) The occurrence frequency increases with the decrease in latitude in the northern and southern hemispheres.

(vi) The height of occurrence is higher during the equinox than the solstice months. The average drift velocity is higher during the equinox months than the solstice months. Low or negative average drift velocity were recorded during the spread F non-occurrence days. Earlier occurrence is noticed during the equinox months while first appearance was noticed in the late hours during the solstice months. Layers begin to rise around 1800LT – 1900LT in most of the stations and rises earlier in the equinox months. Continuous and noticeable increase in virtual height triggered SF and there must be Taylor (R-T) instability to cause the irregularity. Low initial virtual height during the occurrence period is factor that is, low initial virtual height during the occurrence period require high average drift velocity to push it to height of occurrence. Virtual height characteristic during time of occurrence, high value of average drift velocity shows how consistent and regular continuous increase in virtual height towards occurrence window. Low or negative value of average drift velocity shows inconsistent increase or decrease in virtual height towards occurrence window or high initial victual height and height of occurrence/ and few number of the drift.

(vii) It triggered in ILR SEPT between 2030LT and 2145LT and in ILR June is between 2030LT and 2245LT High value of average drift velocity shows how consistent and regular continuous increase in virtual height towards occurrence window. Low or negative value of average drift velocity shows inconsistent increase or decrease in virtual height towards occurrence window or high initial victual height & height of occurrence/ and few number of the drift. Spread F does not occur every night and it is a post sunset affair. Late night spread F occurrence due to the upward drift velocities raise the F layer, make the bottomside to be ExB unstable, and leads to the production of initially weak plasma irregularities.

4.2. Significance of the Study

As a result of the problems that arise in radio communication network due to equatorial spread F, a proper understanding of the statistical occurrence and latitudinal variation of equatorial spread F is of vital importance in radio communication network and design. In order to mitigate these challenges, the effects of these irregularities have been studied extensively. Equatorial spread F study has significant and important benefits in applied research and science. This study has given new valuable information to telecommunication operators and vendors. The results obtained from this study be incorporated into models e.g. international reference ionosphere. Which are used in the design of communication technology.

4.3. Contribution to Knowledge

There are limited published works on spread F occurrence in the African sector and not much has been done in the investigation of spread F occurrence with respect to time and vertical drift velocity. Because of this knowledge gap, the data used for this work includes data from Ilorin station which has not been used before for such study.

4.4. Recommendations

It is recommended that the result obtained in this study be incorporated in the prediction model used in the planning of radio communication links.

REFERENCES

Aarons, J., (1993). The longitudinal morphology of equatorial F-layer irregularities relevant to their occurrence, *Space Sci., Rev.*, 63, 209.

Aarons, J. and Basu, S., (1994). Ionospheric amplitude and phase fluctuations at the GPS Frequencies. *In Proceeding of ION GPS-94, Inst. of Navig., Arlington, Va.,* 1569–1578.

Abdu, M. A., Sobral, J. H. A., Batista, I. S., Rios, V. H., and Medina, C., (1998) Equatorial spread-F occurrences statistics in the American longitudes: Diurnal, seasonal and solar cycle variations, *Adv. Space. Res.*, 22, 851–854.

Abdu, M. A., Jayachand1ra, p. T., MacDouga, n, j., Cecile1,j . F., .Sobra, J .H . A.,(1998).

Equatorial F region zonal plasma irregularity drifts under magnetospheric disturbances. *GEOPHYSICAL RESEARCH LETTERS*, VOL. 25, NO. 22, PAGES 4137-4140, NOVEMBER 15. http://onlinelibrary.wiley.com/doi/10.1029/1998GL900117/pdf

Abdu, M.A., Sastri, J.H., Luhr, H., Tachihara, H., Kitamura, T., Trivedi, N.B. and Sobral, J.H.A. (1998). DP 2 electric field fluctuations in the dusk-time dip equatorial ionosphere. *Geophysical Research Letters 25: doi: 10.1029/98GL01096. issn: 0094-8276.*

Abdu, M. A. (2001). Outstanding problems in the equatorial ionosphere thermosphere electrodynamics relevant to spread F. *J. Atmos. Sol. Terr. Phys.,* 63, 869–884

Abdu M., A., (2012). Equatorial spread F development and quiet time variability under solar minimum conditions. *Indian Journal of Radio & Space Physics. Vol 41*, April 2012, 168-183

Adebiyi, S.J., Adeniyi, J.O., Adimula, I.A., Joshua, B., Gwani, M., (2012). Effect of the geomagnetic storm of April 5th–7th, 2010, on the F2-layer of the ionosphere of Ilorin, Nigeria. World *J. Eng. Pure Appl. Sci.* 2 (2), 56–62.

Adebiyi S.J, (2010). Variation of total electron content during quiet and disturbed conditions in the african-european sector. A thesis submitted in partial fulfillment of the requirement for the Doctor of Philosophy degree in Physics University of Ilorin, Nigeria.

Adebesin, B. O., Adeniyi, J. O., Adimula, I.A., and Reinisch, B.W., (2013). Equatorial vertical plasma drift velocities and electron densities inferred from ground-based ionosonde measurements during low solar activity. *Journal of Atmospheric and Solar-Terrestrial Physics*, **97**, 58–64.

Adebesin, B.O., Adeniyi, J.O., Adimula, I.A., Reinisch, B.W., and Yumoto, K., (2013b). F2 layer characteristics and electrojet strength over an equatorial station, *Advances in Space Research*, **52**, 791 – 800.

Adimula, A. B., (2013) the mandate: the radio as an instrument of dominion. (Inaugural Lecture) https://www.unilorin.edu.ng/UIL/129.pdf

Adeniyi, J. O. (2007). Subduing the earth: the ionosphere inclusive *(Inaugural Lecture)* United Nations Educational, Scientific and Cultural Organization And International Atomic Energy Agency, the Abdussalam international centre for theoretical physics, IC/2007/009, Available at: http://publications.ictp.it

Adeniyi, J.O, Agunbiade, G, Oladipo, O.A., Olawepo, A.O., Adimula, I.A., Reinisch, B.W., McHarg, M.G., Ikubanni, S.O. (2017). Low Latitude Spread-F Occurrence during June Solstice and September Equinox of Sunspot Minimum, the African Review of Physics 12: Special Issue on Applied Physics in Africa 0004

Aggson, T. L., H. Laakso, N. C. Maynard, and R. F. Pfaff. (1996). In situ observations F bifurcations of equatorial bubbles J. *Geophys R.es*., 101, 5125, 1.

Agunbiade, G, Adeniyi, J.O, Oladipo, O.A., Olawepo, A.O., Adimula, I.A., Reinisch, B.W., McHarg, M.G., Ikubanni, S.O. (2015). Low latitude spread-F occurrence during June solstice and September Equinox of sunspot minimum. URSI-NG Conference Proceedings.

Akbar, A. J., Ayub Khan, M.Y. Z., Faisal, A. K. A., Khusro, M., Syed N, A., (2013). Seasonal Variability in Virtual Height of Ionospheric F2 Layer at the Pakistan Atmospheric Region. *Proceedings of the Pakistan Academy of Sciences* 50 (2): 151–158.

Alex, S., P. V. Koparkar, and R. G. Rastogi, Spread-F and equatorial ionization anomaly belt, J. Atmos. Terr. Phys., 51,371-379, 1989.

Alfonsi, L., Spogli L., Pezzopane, M., Romano V., Zuccheretti E., De Franceschi G., Cabrera, M. A., Ezquer R. G.., (2013).Comparative analysis of spread-F signature and GPS scintillation occurrences at Tucumán, Argentina. Journal of Geophysical Research: Space Physics, Vol. 118, 4483–4502, doi:10.1002/jgra.50378. http://onlinelibrary.wiley.com/doi/10.1002/jgra.50378/full

Anderson, D., Anghel, A., Yumoto, K., Ishitsuka, M., and Kudeki, E. (2002). Estimating Daytime vertical ExB drift velocities in the equatorial F-region using ground-based magnetometer observations, Geophys. Res. Let., 29 (12), 1596, doi: 10.1029/2001GL014562.

Anderson, D., A. Anghel, J. Chau, and O. Veliz (2004). Day time vertical EXB drift velocities inferred from ground based magnetometer observations at low latitudes, Space Weather, 2, S11001, doi: 10.1029/2004SW000095.